Annu. Rev. Fluid Mech. 1999. 31:537–66

COLLAPSE, SYMMETRY BREAKING, AND HYSTERESIS IN SWIRLING FLOWS

Vladimir Shtern and Fazle Hussain
Department of Mechanical Engineering, University of Houston, Houston, Texas 77204-4792; e-mail: mece21w@jetson.uh.edu

KEY WORDS: swirl accumulation, vortex breakdown, fold catastrophe, axisymmetry breaking, conical similarity solutions

ABSTRACT

The paper reviews striking features of swirling flows—collapse, swirl generation, vortex breakdown, hysteresis, and axisymmetry breaking—and the mechanisms involved with the help of conical similarity solutions of the Navier-Stokes equations. The strong accumulation of axial and angular momenta, observed in tornadoes and flows over delta wings, corresponds to collapse, i.e. the singularity development in these solutions. Bifurcation of swirl explains the threshold character of swirl development in capillary and electrovortex flows. Analytical solutions for fold catastrophes and hysteresis reveal why there are so few stable states and why the jump transitions between the states occur—features typical of tornadoes, of flows over delta wings, and in vortex devices. Finally, the divergent instability explains such effects as the splitting of a tornado and the development of spiral branches in tree and near-wall swirling flows.

1. INTRODUCTION

Of the many unresolved features of swirling flows, we review a few that seem the most striking: collapse, swirl generation, vortex breakdown, hysteresis, and axisymmetry breaking.

Collapse corresponds to an accumulation of swirl, which occurs in cosmic jets (Lada 1985), in tornadoes (Davies-Jones 1983), on delta wings of aircraft (Menke & Gursul 1997), and even in liquid menisci of electrosprays. Strong accumulation of angular and axial momenta sometimes manifests as a singularity

0066-4189/99/0115-0537$08.00

development (collapse) and a loss of solution in mathematical models of these flows (Section 2).

Swirl generation, discussed in Section 3, seems at first glance to contradict conservation of angular momentum. However, there are examples in everyday life of swirl development without any obvious forcing, e.g. the whirlpool in a bath sink. Whether the bathtub vortex occurs due to symmetry breaking or external forcing has been widely discussed but not resolved (e.g. see Ogawa 1992). Rotation appears as the speed of a swirl-free flow exceeds some threshold in many experimental studies, for example sink flow in a rectangular container (Kawakubo et al 1978), free convection in a sealed cylinder (Torrance 1979), a horizontally oscillating glass of water (Funakoshi & Inoue 1988), an electrically driven flow of mercury in a cup (Bojarevics et al 1989), and the Taylor menisci (Fernandez de la Mora et al 1991).

Vortex breakdown is an abrupt change in the core of a slender vortex and typically develops downstream into a recirculatory "bubble" or a helical pattern. Vortex breakdown is observed in both open flows (e.g. tornadoes and over delta wings) and confined flows (e.g. in cylindrical containers). Despite four decades of extensive studies, there is no consensus on the notion of vortex breakdown, let alone its mechanism (Section 4). A recent view is that vortex breakdown is a fold catastrophe that causes a sudden transition to a different flow state.

Hysteresis and the corresponding finite-amplitude instability are typical of swirling flows, occurring in tornadoes (Burggraf & Foster 1977), above delta-wing aircraft (Lowson 1964), in diverging tubes (Sarpkaya 1971), and in vortex chambers (Goldshtik 1990). If two (or more) stable flow states exist for the same conditions, a finite-amplitude disturbance can cause switching between them. A gradual increase or decrease of control parameters can also cause jumps (Section 5). Such jumps are difficult to predict and can be dangerous (e.g. for aircraft).

Axisymmetry breaking is also of fundamental and practical interest, e.g. the splitting of tornadoes and the transformation of an upstream axisymmetric flow into one- or multihelix patterns through helical vortex breakdown (Sarpkaya 1971). Typically observed when a swirling flow diverges and decelerates, axisymmetry breaking can also occur in a converging flow (Section 6).

In contrast to the above-discussed features, which involve purely inertial mechanisms, the Ranque effect—separation of an isothermal fluid into hot and cold streams—typically involves compressibility (Fulton 1950). A recently discovered enigmatic phenomenon of swirling flows is "antidiffusion": Small particles, initially uniformly distributed in a fluid, leave some (odd-shaped) regions as rotation starts (Husain et al 1995). This review does not address the Ranque and antidiffusion effects, but focuses on single-phase incompressible flows.

Although these striking features have been observed in natural and technological flows as well as studied in laboratory experiments, they are far from being well understood. The main difficulties are the large number of control parameters involved and the sensitivity of the swirling flow to external disturbances. Direct numerical simulations (DNS) of the Navier-Stokes equations (NSE) are subject to the same problems, in addition to technical difficulties associated with complex flows and boundary conditions. In addressing such complex flows, the physical and numerical experiments often include simple models to interpret the observed effects and to explain their mechanisms. Similarity solutions, being mathematical tools for such simplification, help to achieve these goals.

Analytical solutions and semi-analytical methods [which reduce NSE to ordinary differential equations (ODE)] retain the key features of practical flows while omitting secondary features. Flows are typically oblivious of fine details of boundaries, but depend strongly on invariant characteristics such as the flow force and circulation. These two facts together justify, and help obtain, similarity solutions for these flows. The similarity approach also allows us to study the spatiotemporal nonlinear development of (nonsimilar) growing disturbances (Section 7).

There are two broad classes of similarity solutions of NSE—the von Kármán and conical flows—that retain both convective and diffusion terms in ODE. These nonlinear ODE allow description of many important features of practical flows, including development of boundary layers, inner viscous layers, flow separation, as well as the phenomena discussed in this paper. Zanderbergen & Dijkstra (1987) and Goldshtik & Yavorsky (1989) reviewed many interesting effects of the von Kármán class, such as multilayer flows between disks, solution nonuniqueness, and swirl bifurcation. However, the von Kármán similarity, in which the swirl velocity is proportional to the distance from the axis, is limited to axisymmetric flows.

In this review, we focus on conical flows wherein velocity is inversely proportional to the distance from the axis and can depend on the azimuthal angle as well. The striking physical effects discussed above correspond to paradoxical features of their mathematical models. For example, collapse corresponds to the development of a singularity and loss of solution (discussed in Section 2).

2. COLLAPSE

Taylor (1950) considered interaction of a half-line vortex of circulation Γ_d with a normal no-slip plane (endwall) to model a swirl atomizer of a liquid fuel. He found that near the endwall, a converging jet develops that is crucial for the device because practically all the fuel flows near the wall. To obtain a boundary

layer solution describing the jet, Taylor conjectured that boundary layers for the radial and swirl velocities have the same thickness; Cooke (1952) obtained another solution free from this limitation.

The wall jet is driven by the radial pressure gradient; in swirling flows, pressure increases from the axis to the periphery to balance the centrifugal force. Near a normal wall (where swirl is suppressed by the no-slip condition), this pressure gradient induces a radial jet (directed to the axis). Such a wall effect is highly undesirable in vortex technology, because particles (say of catalyst or nuclear fuel) held in rotation inside the chamber by centrifugal forces can be transported by the wall jet to the central orifice and lost.

Goldshtik (1960) tackled this effect while developing a vortex nuclear reactor, reconsidered the vortex-wall problem using the full NSE, and obtained results, in some sense contradictory to Taylor's and Cooke's solutions, as explained below.

The problem has a conical similarity with

$$\mathrm{v_r} = -\nu\psi'(x)/r, \quad \mathrm{v}_\theta = -\nu\psi(x)/(r\sin\theta), \quad \mathrm{v}_\phi = \nu\Gamma(x)/(r\sin\theta),$$

$$p = p_\infty + \rho\nu^2 q(x)/r^2, \quad \Psi = \nu r\psi(x), \quad x = \cos\theta, \tag{1}$$

where (r, θ, ϕ) are the spherical coordinates (Figure 1), $(\mathrm{v_r}, \mathrm{v}_\theta, \mathrm{v}_\phi)$ are the velocity components, p is the pressure, Ψ is the Stokes stream function, ρ is the fluid density, and ν is the kinematic viscosity. The only control parameter is the swirl Reynolds number, $Re_\mathrm{s} = \Gamma_\mathrm{d}/\nu$.

Goldshtik discovered and proved the following surprising feature: The similarity solution exists for $Re_\mathrm{s} < 4 < Re_\mathrm{co}$, but not for $Re_\mathrm{s} > 8 > Re_\mathrm{co}$. Guilloud

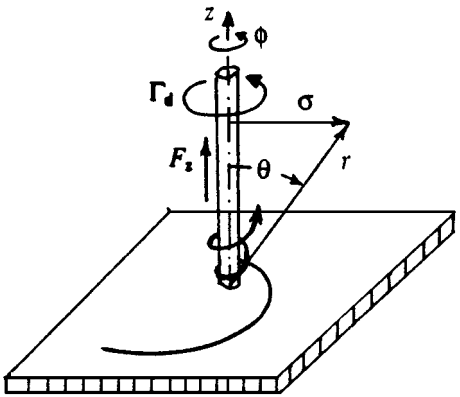

Figure 1 Schematic of the vortex-wall problem. Γ_d is the vortex circulation and F_z is the force along the z-axis.

et al (1973) calculated the exact collapse value: $Re_{co} = 5.53$. The boundary layer approach, applicable for $Re_s \to \infty$, seems invalid because there is no solution for $Re_s > Re_{co}$. The reason for the solution loss is the development of a singularity on the axis as $Re_s \to Re_{co}$—a paradoxical effect for a viscous fluid. One would expect singularities to appear in the limit as Reynolds number goes to infinity, but not at a finite Re_s. The Goldshtik paradoxical example is not unique: Similar collapses of solutions have been found in Marangoni convection (Bratukhin & Maurin 1967), electro-vortex flows (Sozou 1971), and thermal convection (Goldshtik & Shtern 1993).

Serrin (1972) applied the vortex-wall model to tornadoes. To avoid collapse, he generalized the problem by introducing an additional source of motion—force $F_z = 4\pi\rho\nu^2 r^{-1} A$ acting along the axis, where A is a dimensionless characteristic of the force. Figure 1 is a schematic of the line vortex and a typical streamline. Figure 2 is a map of the flow patterns (the insets show the meridional motion) on the parameter plane ($k = Re_s/2$, $P = 1 + 4ARe_s^{-2}$). Serrin found that the solution exists for arbitrarily large Re_s, provided A is properly chosen. However, the collapse paradox remains unresolved because such a solution describes descending flow (*inset A*) or two-cell flow (*B*), but not ascending flow (*C*): There is no solution to the right of curve *F* and line *Co* in

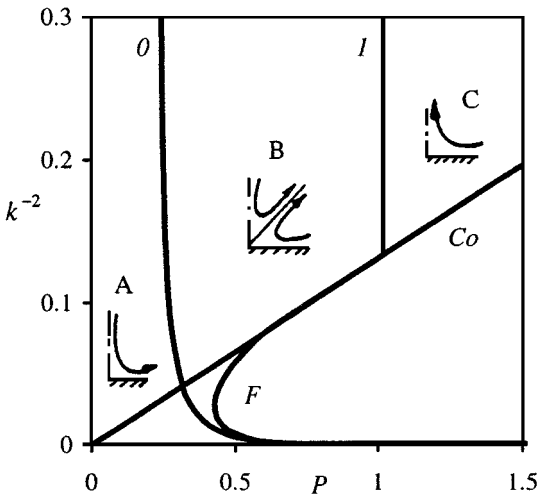

Figure 2 Map of solutions for the vortex-wall problem. Solution is unique above line *Co* while below *Co* there are two solutions to the left of fold curve *F* and no solution to the right of *F*. *Insets A, B,* and *C* show the patterns of the meridional motion in the regions separated by curves *0* and *1*. Below *Co*, the region B is twofold: the region between curves *0* and *F*, and the region between *Co* and *F*.

Figure 2. Serrin mentioned that he had failed to prove the uniqueness theorem. Goldshtik & Shtern (1990) showed that the solution is indeed nonunique: F is a fold curve where two regular solutions merge and disappear (discussed in Section 5), whereas collapse occurs along line Co, $k^{-2} = 0.131P$. Thus, there are two different mechanisms of the solution loss—collapse and fold—and only one (collapse) corresponds to the singularity development.

The physical reason why collapse can occur only in the ascending flow is that such a flow converges toward the axis, transports axial and angular momenta, and dominates the opposing action of viscous diffusion when Re_s is large. As a result, swirl becomes locked along the axis (with no swirl outside), where the axial velocity increases. Thus, the vortex-wall interaction causes self-focusing of swirl and formation of a strong ascending jet—features typical of tornadoes. One expects the accumulation to develop asymptotically as $Re_s \to \infty$, while surprisingly, the singularity occurs at finite Re_s.

This paradox disappears if the flow domain does not include the axis, e.g. when the force and circulation, given on the surface of a narrow cone, induce a flow between the cone and the wall (Goldshtik & Shtern 1990). In such flows as well as in two-cell flows shown in *inset B*, Figure 2, a near-wall boundary layer develops as $Re_s \to \infty$; this converging jet develops in a manner similar to that predicted by Taylor. However, in contrast to the Taylor (1950) and Cooke (1952) solutions, no boundary layer for swirl exists near the wall because the meridional flow "locks" swirl along the cone.

In the vortex-wall model, a line vortex is located on the axis, i.e. there is a singularity in the problem formulation. However, collapse also occurs in thermal convection and in electro-vortex flows where no singularity is imposed on the axis. The solution for the Marangoni convection coincides with that obtained by Yatseev (1950) and Squire (1952):

$$\psi = 2\alpha(1-x)[(1+x)^n - (1+x_c)^n]/[a-(1+x)^n] \qquad \text{for } C < 1/2, \tag{2a}$$

$$\psi = (1-x)/\{2/\ln[(1+x)/(1+x_c)] - 1\} \qquad \text{for } C = 1/2, \tag{2b}$$

$$\psi = 2C(1-x)/\{\omega\cot(1/2\omega\ln[(1+x)/(1+x_c)]) - 1\} \quad \text{for } C > 1/2. \tag{2c}$$

Here $\alpha = (1+n)/2$, $a = (1+x_c)^n(1+n)/(1-n)$, $\omega = in$, $n = (1-2C)^{1/2}$, and $Re = -C(1-x_c)/(1+x_c)$, where Reynolds number $Re = rv_{rc}/\nu = -\psi'(x_c)$ is based on the radial velocity at the conical surface $x = x_c$ ($x_c = 0$ for the plane).

Equation 2 explicitly shows the mathematical reason for the collapse: The denominator in Equation 2c becomes zero at a certain $\underline{Re} = \underline{Re}_{co} < 0$, $\underline{Re} = -Re$ (a negative Re corresponds to flow convergence near the surface, hence $\underline{Re}$ is positive). This solution has a number of applications although, initially, its physical interpretation encountered some difficulties. Yatseev supposed that Equation 2 had no physical meaning. Squire interpreted this equation, for the particular case $x_c = 0$, as a jet emerging normal to a plane wall, but Schneider et al (1987, see also references therein) found that Squire's interpretation is wrong. Relevant applications of Equation 2 are flows driven by shear stresses on a nonrigid boundary. An example is the Marangoni convection (Bratukhin & Maurin 1967). Wang (1991) used Equation 2 with $Re > 0$ to model a flow driven by oil spreading on the ocean surface after an oil spill. Shtern & Barrero (1995) applied the equation for a flow inside conical menisci of electrosprays.

There are also other applications of Equation 2. One can imagine a water film flowing on a horizontal plane toward a sinkhole and forcing a converging motion of air above. If the sinkhole is filled with water, air must turn upward and develop into a vertical jet above the hole, a motion that can be modeled by this equation. An analogous and more interesting application is in modeling cosmic jets, where the highly dense matter of accretion disks acts as the water film while a low-density ambient gas behaves like the air (Goldshtik & Shtern 1993). When there is a vortex-sink of water, the air motion becomes swirling. Goldshtik (1979) and Yih et al (1982) generalized Equation 2 for such swirling flows where circulation is also given on the surface $x = x_c$. Collapse occurs in these solutions as well, and $\underline{Re}_{co}$ increases with swirl (Goldshtik & Shtern 1990).

Thus, collapse at $Re = Re_{co}$ corresponds to a clear physical process: the strong accumulation of the axial and angular momenta. However, in practical flows, $\underline{Re}$ can be larger than $\underline{Re}_{co}$; this requires interpretation by mathematical modeling. One scenario is that the corresponding solution becomes unstable for $\underline{Re} < \underline{Re}_{co}$, resulting in bifurcation into new solutions that exist also for $\underline{Re} > \underline{Re}_{co}$. We show examples of such instability and bifurcation in Sections 3 and 6.

An alternative scenario of fundamental interest is the change in the velocity dependence on r. Collapse occurs in solutions for an unbounded flow region. In a confined, viscous flow, with a finite velocity given at its boundary, no singularity can occur inside the region. Consider a source of motion of dimension r_i (r_i can be the nozzle radius) and a flow region of dimension r_o (r_o can be the distance from the nozzle to a wall). A similarity solution can approximate such a flow only in some range $r_i < r < r_o$. For example, far from a nozzle and a wall, both the mean and fluctuating velocities have conical similarity, $v \sim 1/r$, in turbulent jets (Wygnanski & Fiedler 1969). Schlichting (1933) or Landau (1944) solutions can model the mean velocity of such a flow. [These solutions

exist at arbitrarily large Re, but differ (even in the limit $Re \to \infty$) from inviscid jets, where velocity is r-independent. Goldshtik (private communication) pointed out that this difference in the r-dependence of the viscous and inviscid jets needs to be explained.]

Consider a steady axisymmetric flow describing the Marangoni convection induced by a small heat sink located at the center of the free surface of a liquid in a hemispherical container. The solution described by Equation 2 approximates this flow for $\underline{Re} < \underline{Re}_{\rm co}$, but does not exist for $\underline{Re} > \underline{Re}_{\rm co}$. How do features of the bounded flow change as $\underline{Re}$ passes $\underline{Re}_{\rm co}$? One possibility is that the flow has no similarity region for $\underline{Re} > \underline{Re}_{\rm co}$. Another is that two similarity regions exist having different power laws: $\mathrm{v} \sim r^{-\mathrm{n}}$ with $n = 1$ outside the vicinity of the axis and $n < 1$ inside. As $\underline{Re}_{\rm co} \to \infty$, n can tend to zero, providing a smooth transition from the viscous to inviscid solutions. A similar problem, concerning the similarity and bounded-region solutions, appears in electrovortex flows (Bojarevics et al 1989). Note that in contrast to NSE, the boundary layer equations admit similarity solutions with $n \neq 1$ (e.g. see Fernández-Feria et al 1995). It would be instructive to obtain a steady axisymmetric solution in a bounded region (using DNS) and to investigate its features as Re increases. Bojarevics et al (1989) did such calculations and found that the bounded-region and similarity solutions are alike for moderate Re; the flow features for large Re remain unresolved. This scenario and the r-dependence require further study (Section 8 lists some unresolved problems).

3. SWIRL GENERATION

The collapse paradox—loss of solution at $\underline{Re} = \underline{Re}_{\rm co}$—is overcome if we consider bifurcation of new solutions for $\underline{Re} < \underline{Re}_{\rm co}$. We treat here instabilities leading to bifurcations: (*a*) appearance of swirl in swirl-free flows, (*b*) hydromagnetic dynamo, and (*c*) axisymmetry breaking. Among these effects, (*a*) ("swirl dynamo") seems the most intriguing, since it appears to violate conservation of angular momentum. For (*a*) to occur, either a separation mechanism of angular momentum or swirl-source activation must come into play at critical values of control parameters. Both these mechanisms occur under certain conditions.

The separation takes place owing to growing disturbances, which generate clockwise and counterclockwise swirls in different flow regions with zero net (volume integrated) value of the angular momentum. A part of the momentum diffuses to infinity or to a wall, and thus the compensating momentum appears nonzero in a secondary flow state resulting from the instability. Goldshtik et al (1984) found such a mechanism in a submerged, round jet with a top-hat velocity profile. For supercritical Reynolds numbers ($Re > Re_{\rm cr}$), growing helical oscillations of the azimuthal wavenumber $m = \pm 1$ (Batchelor &

Gill 1962) generate opposite swirls near the jet axis and the periphery. After the nonlinear saturation of these disturbances, the secondary state has a net angular momentum, which can be clockwise or counterclockwise depending on initial conditions. A serious limitation of the round jet case is the parallel flow approximation used for studying stability and bifurcation. Whether such a self-rotation phenomenon would occur in real nonparallel jets remains unclear.

Sagalakov & Yudintsev (1992) considered another flow, which is free of this drawback. An electrically conducting fluid moves in an annular pipe in the presence of an axial magnetic field. While bifurcation of oscillatory solutions is subcritical in nonmagnetic channel flows, a sufficiently strong magnetic field makes bifurcation supercritical. Again for $Re > Re_{cr}$, two growing helical oscillations exist, which saturate to one of two stable states with the time-mean swirl having opposite directions near the inner and outer walls. The net angular momentum of the secondary flow is not zero, because the pipe absorbs the compensating momentum during the saturation process. The separation mechanism of such a swirl generation is rather sophisticated in that it involves two three-dimensional time-dependent disturbances and three secondary flow states: two with opposite signs of swirl and a swirl-free oscillatory solution, which is unstable. The time-mean secondary state includes counterrotation, which results from diffusion of the angular momentum to ambient space or to the walls, and the nonlinear effect of helical oscillations.

The second mechanism—swirl-source activation—also requires thorough physical interpretation, but its mathematical model is simpler than that for the separation mechanism. Also, the secondary states are simpler, having no counterrotation and being steady and axisymmetric, similar to the primary, swirl-free flow. The axisymmetry indeed posed some difficulty in the finding and interpreting the swirl bifurcation. In axisymmetric flows, there are strong constraints for the self-generation of swirl and magnetic field (swirl and hydromagnetic dynamo are analogous in both their mechanism and formalism). These constraints follow from the Cowling-Braginsky theorem: The axisymmetric hydromagnetic dynamo cannot occur.

Cowling's proof (1934) is based on clear physical reasons for secondary states with closed magnetic lines. Braginsky (1964) proposed a different (more formal) proof, using the requirement that magnetic induction decays as r^{-3} or faster as $r \to \infty$. A similar "antidynamo" theorem can be proved easily for swirl generation as well. However, both conditions—the fast decay and the closed lines—are invalid for conical flows, where magnetic and stream lines are open, and magnetic induction and velocity are proportional to r^{-1}. Therefore, bifurcation of swirl and magnetic field in conical flows does not contradict the antidynamo theorem. Moreover, it can be proved that such a bifurcation must occur under certain conditions, as explained below.

The simplest (physically and mathematically) case is bifurcation of swirl in liquid cones. Zeleny (1917) found that the meniscus of a conducting liquid at the exit of a capillary tube takes a conical shape when the liquid is charged to a sufficiently high voltage. Taylor (1964) explained that this shape results from the balance between the electrical pressure and surface tension effects when the liquid is at rest. Very near the cone apex, the liquid surface breaks and a thin jet or spray erupts whose diameter may be more than a thousand times smaller than the inner diameter of the capillary tube (Fernández de la Mora 1992). In recent years, this phenomenon has drawn wide attention because of a rapidly growing area of electrospray applications—from spray painting and jet printing to fuel atomization and biotechnology (Bailey 1988, Fenn et al 1989). As a result, striking new features have been revealed.

In contrast to earlier conjectures that the flow inside the cone is always unidirectional, experiments have revealed a circulatory meridional motion (Hayati et al 1986). For liquids of small conductivity and viscosity, this circulation is driven by electrically induced surface stresses $\tau_{\theta \mathrm{r}} = \varepsilon_0 \mathrm{E}_\theta \mathrm{E}_\mathrm{r}$. Here ε_0 is the vacuum permittivity, while E_θ and E_r are the normal and tangential components of the electric field at the liquid surface, respectively. As the voltage increases up to 5.5 kV, swirl appears and becomes so strong that a kind of microtornado develops within the tiny (1 mm) meniscus. A microscope reveals how this tornado undergoes vortex breakdown: First, a recirculatory bubble appears; it then expands upstream and downstream and assumes a conical form (Shtern & Barrero 1995). A simple similarity model predicts both the swirl generation and the development of the recirculatory zone.

In the linear stability problem for swirl disturbances of conical flows, the equation for circulation Γ reduces to $(1 - x^2)\Gamma'' = \psi\Gamma'$, where ψ is given by Equation 2. Integrating twice and using the normalization $\Gamma(x_\mathrm{c}) = 1$ and the boundary condition that the swirl shear stress is zero (i.e. $\tau_{\theta\phi} = 0$) at the cone surface, $x = x_\mathrm{c}$, yields the relation

$$\Gamma(1) \equiv \Gamma_1 = 1 - 2x_\mathrm{c}\left(1 - x_\mathrm{c}^2\right)^{-2} \int U^{-2} dx, \tag{3}$$

where the integration is from x_c to 1; and the function $U(x)$, lying in the range $0 < U(1) \le U \le U(x_\mathrm{c}) = 1$, depends only on ψ. As $Re \to Re_\mathrm{co}$, $U(1)$ tends to 0.

For bifurcation to occur, Γ_1 must be zero. It is evident from Equation 3 that $\Gamma_1 > 0$ for $x_\mathrm{c} \le 0$, and therefore the swirl dynamo is impossible for a cone angle $\theta_\mathrm{c} \ge 90^\circ$. At $Re = 0$, $U \equiv 1$ and Equation 3 yields $\Gamma_1 = (1 - x_\mathrm{c})/(1 + x_\mathrm{c}) > 0$. Therefore, the dynamo cannot occur in a slow flow. On the other hand, as Re approaches Re_co, the integral in Equation 3 tends to infinity and Γ_1 is negative. Since Γ_1 is a continuous function of Re, there must be a specific $Re = Re_\mathrm{cr}$, at

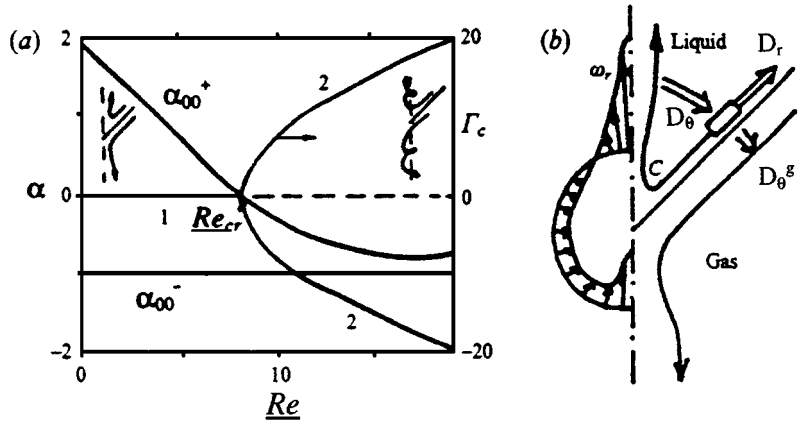

Figure 3 (*a*) The pitchfork bifurcation of swirl (curves *1* and *2*) and the leading eigenvalues α_{00}^{+} and α_{00}^{-} versus Reynolds number $\underline{Re}$ for the electrospray flow. *Insets* sketch the primary and secondary flows. (*b*) Schematic of the angular momentum fluxes (*right-hand side*) and of the radial vorticity distribution (*left-hand side*).

which $\Gamma_1 = 0$ and the swirling flows bifurcate. Calculations yield, for example, $\underline{Re}_{\rm cr} = 6.3$ for $x_{\rm c} = 0.707$ (i.e. for the cone angle $\theta_{\rm c} = 45^\circ$). This proof of swirl bifurcation explains the threshold character of the swirl appearance in the experiment.

Bifurcation study (Shtern & Barrero 1995) and analysis of instabilities to steady and slowly time-varying disturbances (Shtern & Hussain 1998) illuminate the mechanism of swirl accumulation. Figure 3*a* shows the results obtained for the flow of heptane inside, and air outside, the $\theta_{\rm c} = 45^\circ$ meniscus (Figure 3*b*). In Figure 3*a*, α is the spatial growth rate of disturbances, which are proportional to $\exp(\alpha r)$, and $\Gamma_{\rm c} = \Gamma(x_{\rm c})$. Only the modes of smallest $|\alpha|$ are plotted: the curves α_{00}^{+} and α_{00}^{-}. Note that positive α_{00}^{+} indicates that the corresponding outer disturbance (i.e. introduced far away from the cone tip) decays as r decreases for small $\underline{Re}$. The disturbance grows for $\underline{Re} > \underline{Re}_{\rm cr}$ where $\alpha_{00}^{+} < 0$. Line *1* and curve *2* correspond respectively to the primary and secondary flow states and illustrate the supercritical pitchfork bifurcation. The crossing of the line $\alpha = 0$ and the curve α_{00}^{+} indicates instability, resulting in the appearance of swirl.

To explain the mechanism of swirl accumulation, consider the balance of angular momentum for a small, near-interface element of liquid, denoted by the rectangle in Figure 3*b*. Symbol *C* marks convection of angular momentum along a streamline, where circulation would be constant in an inviscid fluid. As the streamline approaches the axis, the swirl velocity and the radial vorticity

ω_r grow. A typical dependence of the radial vorticity on the polar angle θ (for fixed r) is shown on the left-hand side of Figure 3*b*. The sharp peak of vorticity on the axis causes viscous diffusion and hence the angular momentum transfer across streamlines from the axis to the interface (D_θ in Figure 3*b*), resulting in an increase in circulation of the liquid element. The diffusion fluxes in the radial direction, D_r, and from the liquid to the gas, D_θ^g, decrease circulation of the liquid element. The stability calculations for $\underline{Re} < \underline{Re}_{cr}$ show that the losses, $D_r + D_\theta^g$, exceed the gain, D_θ (as expected for low $\underline{Re}$), and therefore Γ_c decreases with decreasing r. However, for $\underline{Re} > \underline{Re}_{cr}$, D_θ dominates $D_r + D_\theta^g$, and Γ_c increases as r decreases, until nonlinear saturation. Saturation results from the centrifugal action of a strong swirl that pushes streamlines away from the axis, whereupon the vorticity decreases along the axis. Therefore, D_θ decreases; it reaches a new balance with $D_r + D_\theta^g$; this balance corresponds to the secondary similarity regime.

The loss of the angular momentum owing to the radial diffusion through the surface, $r = \text{const}$, increases with the cone angle, θ_c. In contrast, as θ_c increases, $d\Gamma/d\theta$ and D_θ decrease; the resulting dominance of losses explains the absence of swirl bifurcation for large θ_c (for $\theta_c \geq 90^\circ$ as theory shows). A large liquid/gas density ratio causes the gas flow to contribute very little to the angular momentum. Therefore, the value of the angle formed by the liquid surface is the only crucial parameter for instability. However, if θ_c is very small, streamlines are nearly parallel to the axis; this decreases the accumulation effect. Thus $\underline{Re}_{cr}$ reaches its minimum at an intermediate θ_c value (near $\theta_c = 45^\circ$ sketched in Figure 3).

Circulation must reach its maximum at the boundary of the flow region for an incompressible fluid with uniform physical properties. This maximum is at the meniscus surface, which is indeed the flow boundary for the single-phase flow. However, the maximum principle is not applicable to a fluid whose properties change in space, and the circulation maximum is located inside the region in the two-phase flow. Another example is the single-phase flow of fluid with variable viscosity (Goldshtik & Shtern 1993), where circulation maximum is located inside the region and swirl bifurcation occurs for $\theta_c \geq 90^\circ$ as well. Thus, a proper stratification of density and viscosity can enhance swirl generation.

The mechanism of the axisymmetric hydromagnetic dynamo (i.e. the appearance of magnetic field due to instability) is similar to that of swirl bifurcation but involves one more important effect: generation of electric current that enhances the instability. Consider a magnetic field perturbation, directed along the axis, and a coaxial toroidal liquid element remote from the axis. A converging flow transports the element toward the axis, crossing magnetic lines and thus generating an azimuthal electric current. This current in turn induces a meridional magnetic field having the same direction near the axis as the original field;

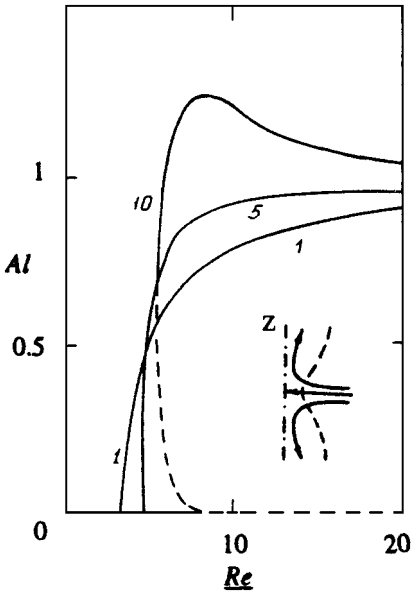

Figure 4 Intensity of the magnetic field, *Al*, vs the Reynolds number *Re* for the hydromagnetic dynamo. As circulation Γ_0 increases (see numbers near the curves), bifurcation transforms from super- to subcritical. *Inset* shows a typical magnetic line (*dashed*) and streamlines of the meridional motion.

such a positive feedback enhances the hydromagnetic instability. This effect explains why, in contrast to the swirl bifurcation, the hydromagnetic dynamo does not have the $\theta_c < 90^\circ$ limitation. This difference is important for application of the model to the development of basically axisymmetric magnetic fields of stars (Goldshtik & Shtern 1993).

Also of interest is the influence of swirl on the magnetic field generation. Figure 4 shows the variation of Alfven number *Al* with *Re* for different values of the circulation $\Gamma_0 = \Gamma(0)$; *Al* is the magnetic/kinetic energy ratio on the equatorial plane, $x = 0$ (this ratio is the same everywhere on the plane). The inset shows a magnetic line (*dashed*) and typical streamlines (*solid*) of the meridional flow induced by a vortex sink at the plane, $x = 0$. Bifurcation of magnetic field is supercritical for small Γ_0 (e.g. $\Gamma_0 = 1$, Figure 4) but subcritical for large Γ_0 (e.g. $\Gamma_0 = 10$). Therefore, in flows with strong swirl, the magnetic field can appear and disappear through jumps as *Re* respectively increases and decreases, i.e. hysteresis occurs.

A common feature of the swirl and magnetic field bifurcations is that there is a remote source of swirl or magnetic field, which does not affect the similarity

region for subcritical $\underline{Re}$ but causes the accumulation effect for supercritical $\underline{Re}$. It is worth noting that the swirl and magnetic field intensity in the secondary state does not depend on, and can be drastically larger than, the source strength. Another common feature is that both the effects occur in flows converging toward the axis of symmetry. While it is not too surprising that a converging flow accumulates swirl and magnetic fields, the threshold character of this effect is nontrivial. This result is in agreement with observations of swirl generation in menisci of electrosprays and in electro-vortex flows. For example, flow of mercury in a hemispherical container forced by the electric current $I < 15$ A is swirl-free, but becomes swirling for $I > 15$ A (Bojarevics et al 1989).

The swirl accumulation causes the pressure in the vortex core to be significantly less than the ambient pressure. If a swirling flow is directed against the pressure gradient, the pressure recovery can trigger another interesting effect—vortex breakdown.

4. VORTEX BREAKDOWN

Owing to the enormous extent of work in this area (see reviews by Hall 1972, Leibovich 1978, Escudier 1987, and Althaus et al 1995), we discuss only key issues and restrict our attention to recent studies. Most of the applications of vortex breakdown (as well as its discovery by Peckam & Atkinson 1957) concern flows over delta wings of aircraft. The upper part of Figure 5 (from flow visualization by Werle 1963) shows the formation of the vortex core above a delta wing (*white strips*). Experiments (Earnshow 1961) reveal that the core is an intense, swirling jet with a sharp peak in the longitudinal velocity, resulting from the focusing of longitudinal momentum and swirl in the roll-up process.

This mechanism is similar to collapse (Section 2) and swirl dynamo (Section 3): Flow separation at the leading edge provides a source of vorticity, which accumulates in the core. The lower part of Figure 5 models this

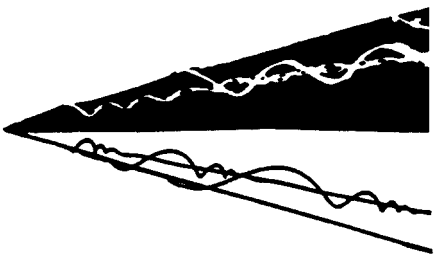

Figure 5 Formation of the delta-wing vortex (*above*, Werle 1963) and its model (Shtern et al 1997).

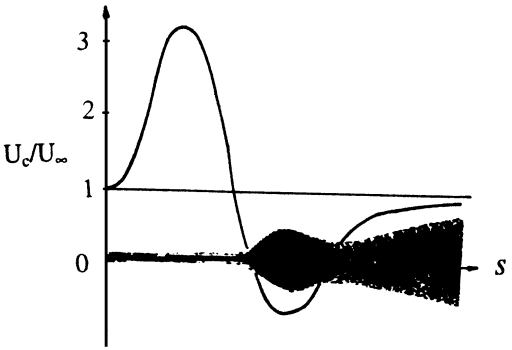

Figure 6 Schematic of dependence of longitudinal velocity U_c at the core axis on the streamwise coordinate s, superimposed with visualization of the bubble-type vortex breakdown (Sarpkaya 1995).

process with the help of an analytical solution of NSE for a vortex-sink with an axial flow (Shtern et al 1997). The mechanism of core formation given by this model is as follows: The roll-up of the separation surface leads to the generation of swirl (as shown by the streamlines in Figure 5). The swirl induces a pressure drop toward the axis, thus attracting other streamlines to the axis; this further focuses the swirl, thereby further decreasing the pressure in the core. This positive feedback leads to the strong accumulation of axial vorticity and momentum, i.e. to the formation of the vortex core.

Downstream, the pressure returns to its ambient value, and the swirling jet decelerates, causing internal flow separation (from the core axis) to occur, resulting in a recirculatory bubble or a helical structure. Figure 6 shows a visualization of the bubble-type vortex breakdown (Sarpkaya 1995) and a sketch of the dependence of the longitudinal velocity, U_c, along the vortex axis s; U_∞ is the free-stream velocity. There are four regions: 1. jet formation, where U_c can increase up to $5U_\infty$ (Menke & Gursul 1997); 2. developed jet, where U_c saturates and starts to decrease; 3. recirculatory bubble, where U_c is negative; and 4. vortex wake, where U_c recovers to U_∞. The wake above delta wings is turbulent but can be laminar in confined swirling flows. Figure 7 shows a picture of two vortex breakdown bubbles in a sealed cylinder with a rotating endwall (Escudier 1984) and their modeling by analytical solutions of NSE (Shtern et al 1997).

Theoretical approaches can be classified into four groups that focus on different facets of vortex breakdown:

1. Collapse of the near-axis boundary layer. The core of a slender vortex is well predicted by parabolized equations, e.g. boundary layer or quasicylindrical approximations of NSE (Hall 1972). The slenderness condition ($a\partial/\partial s \ll 1$,

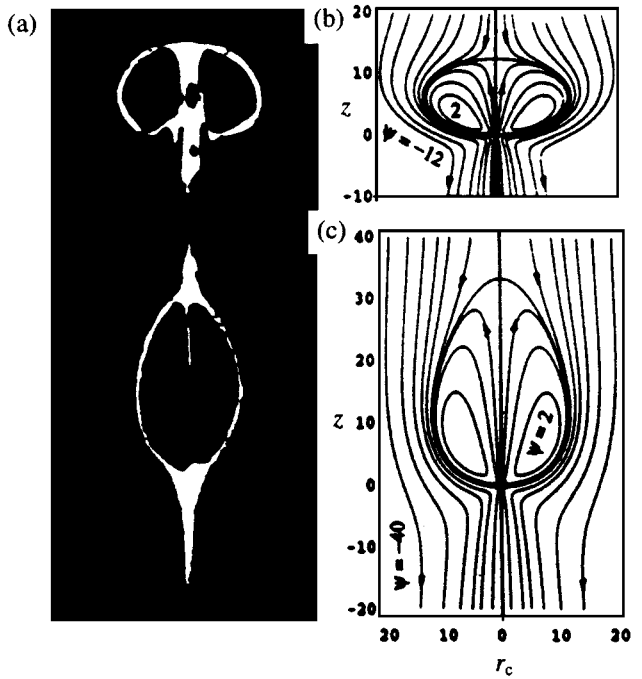

Figure 7 Vortex breakdown in a sealed cylinder (Escudier 1984) and its model (Shtern et al 1997).

where a is the core radius and s is the longitudinal coordinate) becomes invalid as vortex breakdown occurs. The corresponding boundary layer solutions suffer from a singularity in the vicinity of flow separation. This approach captures only the early stages of the core change.

2. Internal flow separation. Some researchers include development of a recirculatory zone and flow reversal in the vortex-breakdown definition (Leibovich 1978). However, the flow reversal and recirculatory zone do not necessarily occur in helical and turbulent vortex breakdowns (Sarpkaya 1995). Leibovich (1984) proposed a model of vortex breakdown as a soliton and the separation zone as the soliton core. A drawback of his approach is that states on either side of a soliton are the same, in contrast to vortex breakdown, where the flow states are very different.

3. Inertial wave roll-up. This theory considers the vortex core as a wave guide and treats vortex breakdown similar to hydraulic jumps (Squire 1956, Benjamin 1962, Keller et al 1985). Although inertial waves play an important role in swirling flows, their application to vortex breakdown has the following

limitations: The wave theory predicts the appearance of a stagnation point with decreasing swirl number while vortex breakdown develops as the swirl number increases in experiments (Sarpkaya 1971). The theory fails to predict the abrupt vortex consolidation observed in swirling flows (Section 5). Benjamin analytically continued the velocity field inside the separation zone, which seems invalid (Wang & Rusak 1997). The stagnation-zone model (Keller et al 1985) also has limitations, which are discussed in Section 5.

4. Instability. The helical vortex breakdown certainly relates to symmetry breaking of the upstream flow and therefore to its instability with respect to spiral disturbances (Leibovich 1984). An advanced stability approach interprets vortex breakdown as a transition from a convective instability to an absolute instability (Olendraru et al 1996, Delbende et al 1998). However, the instability does not necessarily lead to vortex breakdown, and axisymmetric vortex breakdown can occur without instability, as shown for a flow in a sealed cylinder (Gelfgat et al 1996).

Vortex breakdown has also been viewed as a fold catastrophe, discussed in the next Section.

5. HYSTERESIS

Trigub (1985) found that, under certain conditions, the quasicylindrical approximation of NSE has a fold in its solution space, which can be physically interpreted as vortex breakdown. Saffman (1992) and Buntine & Saffman (1995) developed this view by studying inviscid swirling flows and using the analytic approach by Batchelor (1967). They concluded that two regular solutions, both corresponding to unidirectional flows, can merge and disappear as Squire number Sq (inflow swirl/axial velocity ratio) exceeds some value, $Sq_{\rm f}$. As a result, a jump transition must occur at $Sq = Sq_{\rm f}$ to a very different flow state, e.g. with a recirculatory zone.

Such a fold catastrophe provides an alternative scenario of vortex breakdown, compared with the smooth development of separation zone as Sq increases. In the latter case, the axial velocity continuously decreases and changes its sign. Wang & Rusak (1997), Goldshtik & Hussain (1997, 1998), and Rusak et al (1998) further developed the fold-catastrophe approach by studying vortex breakdown in pipes and argued that stagnation zones (rather than recirculatory zones) appear in inviscid flows, as Keller et al (1985) conjectured. DNS of steady NSE solutions for swirling flows in diverging pipes (Beran & Culick 1992, Lopez 1994) also reveal the solution nonuniqueness associated with folds. Lopez (1998) found similar hysteresis for a flow in a rotating, sealed cylinder with a differentially rotating endwall.

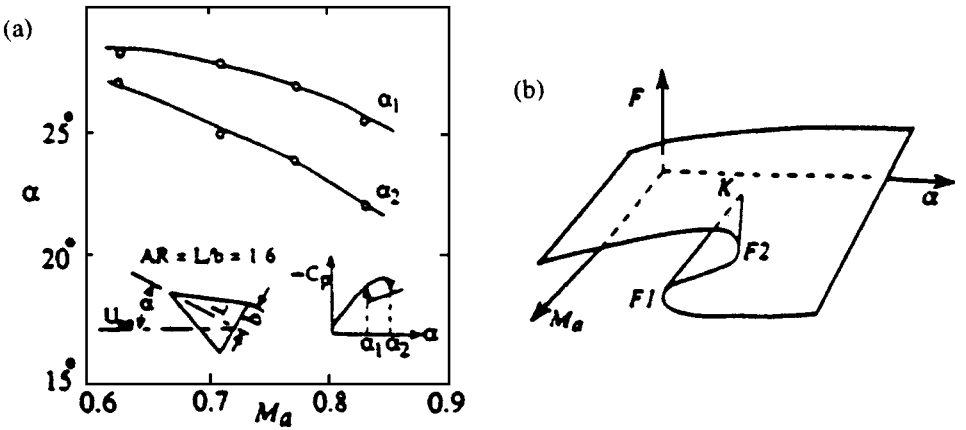

Figure 8 (*a*) Hysteretic transitions for flow above a delta wing (Muylaert 1980), and (*b*) its explanation in terms of cusp (*K*) and fold (*F1* and *F2*) catastrophes.

These interesting theoretical results agree with observations of hysteresis (typical of swirling flows discussed in Section 1) but do not explain the physical reasons for the occurrence of folds. Analytical solutions for conical swirling jets are helpful in achieving this goal. We refer the reader to Shtern & Hussain (1996) for details and consider here a conical model of vortex breakdown, which mimics the effects occurring in tornadoes and delta-wing vortices. While the observations are only occasional in tornadoes (Burggraf & Foster 1977), the hysteresis above delta wings is frequent and has been studied extensively in the laboratory (discussed below).

Figure 8*a* presents results from experiments (Muylaert 1980) involving hysteretic transitions above a delta wing. The insets show the flow schematic and the dependence of the pressure coefficient C_p on the angle of attack α at a fixed Mach number Ma. There are jumps in the value of C_p at $\alpha = \alpha_2$ as α increases and at $\alpha = \alpha_1$ as α decreases. In the range $\alpha_1 < \alpha < \alpha_2$, there are two stable states that have different C_p (i.e. bi-stability). The jumps correspond to abrupt shifts in the vortex breakdown location—downstream at $\alpha = \alpha_1$ and upstream at $\alpha = \alpha_2$. The main plot shows the dependence of α_1 and α_2 on Ma (although compressibility is not essential for hysteresis).

The catastrophe theory is an appropriate mathematical technique to analyze such jumps. Figure 8*b* is a sketch showing the dependence of lift force F on Ma and α corresponding to Figure 8*a*. Surface $F(\alpha, Ma)$ has folds *F1* and *F2*, which meet and terminate at cusp point K (Arnol'd 1984).

The conical model, discussed below, provides an analytical solution describing the folds and also the appearance of the cusp as Re_s increases. Figure 9*a*

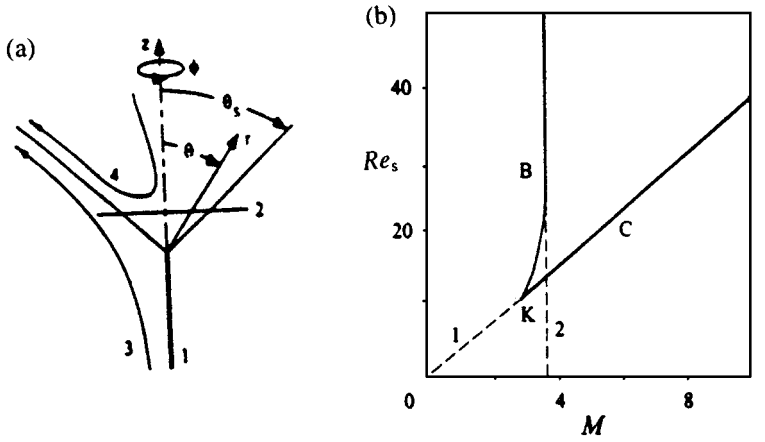

Figure 9 (*a*) Schematic of a model for hysteresis shown in Figure 8. Half-line vortex *1* of circulation Re_s and flow force M (acting on planes sush as *2*) induce a flow, which can have two cells; *curves 3* and *4* show typical meridional streamlines. (*b*) Numerical (*solid*) and analytical (*dashed*) results for folds corresponding to vortex breakdown (*B*) and consolidation (*C*).

shows a schematic of the flow, where half-line vortex *1* models a consolidated vortex core (upstream of the vortex breakdown) and *curves 3* and *4* represent typical streamlines of the meridional motion outside and inside the recirculatory zone bounded by the conical surface, $\theta = \theta_s$. The control parameters are Re_s (dimensionless circulation of the vortex) and $J_0 = J(2\pi\rho\nu^2)^{-1}$, where J is the flow force acting on the normal plane, $z = \text{const} > 0$ (line *2*, Figure 9*a*).

The problem was first studied by Goldshtik (1979) for small Re_s and J_0, followed by Paull & Pillow (1985), who considered a special relation between Re_s and J_0 and found an analytical solution in the limit $Re_s \to \infty$. Sozou et al (1994) obtained two more solutions of the Paull & Pillow problem (thus showing the solution nonuniqueness), and Shtern & Hussain (1996) developed a general theory of hysteresis in swirling jets.

Figure 9*b* shows folds (*curves B* and *C*) and cusp K on the parameter space (M, Re_s), where $M = 2\pi J_0 Re_s^{-2}$. The *solid curves* represent the numerical results, and *lines 1* and *2* are their asymptotes as $Re_s \to \infty$. *Line 2* ($M = 3.74$) corresponds to vortex breakdown in the near-axis Long's jet (Long 1961), and *line 1* depicts the analytical solution for the fold, $M = \pi Re_s/12$ (Shtern & Hussain 1996), in the two-cell flows (Figure 9*a*). The maximum radial velocity, v_{rm}, of the annular jet flowing out along the surface, $\theta = \theta_s$, is independent of θ_s: $rv_{rm}/\nu = Re_s^2/8$.

These asymptotic solutions satisfactorily approximate the flow even for moderate Re_s (Figure 9*b*) and explain the solution nonuniqueness. To show this,

we consider the dependence of J on v_{rm} at fixed Re_s. For the flow consolidated near the axis, the dominant contribution to J is from the momentum flux, $\rho v_{rm}^2 S_j$, where S_j is the area of cross-section of the jet projected on a plane normal to the axis. For the swirl-free round jet, $S_j \sim \delta^2 \sim 1/v_{rm}$ yields $J \sim v_{rm}$ (Schlichting 1933). Therefore, J decreases with v_{rm} when the swirl contribution to the meridional motion is negligible. However, as v_{rm} decreases, the swirl contribution becomes significant (in the vicinity of *fold B* in Figure 9*b*) because centrifugal force spreads the jet and S_j rapidly increases. Since $r v_{rm}/\nu$ asymptotes to the constant, $Re_s^2/8$, as $Re_s \to \infty$, the negligible decrease in v_{rm} cannot compensate for the increase in S_j. Therefore, J starts to increase with further decrease in v_{rm}. Thus the minimum of the flow force in Long's jet (at *fold B*) is a result of the spreading of the jet by swirl. Because of this minimum in J, the transformation of the near-axis jet into a two-cell flow (as the control parameter J_0 decreases) cannot be continuous, and vortex breakdown occurs through a jump.

The second extremum of J (at *fold C*) occurs when θ_s becomes sufficiently large to decrease the projection area. As θ_s approaches 90°, both $S_j \sim 2\pi\delta r \cos\theta_s$ and J approach zero. Therefore, J increases as θ_s starts to increase from zero, but again decreases as θ_s approaches 90°. Thus the maximum of J in the two-cell flow stems from a change in the jet direction: from nearly parallel to nearly normal to the axis. Because of this maximum in J, the transformation of the two-cell flow into a near-axis jet cannot be continuous when control parameter J_0 increases, i.e. vortex consolidation (as well as vortex breakdown) occurs through a jump. Note that the conical model explains both abrupt transitions: vortex breakdown and vortex consolidation.

The conical model helps explain also hysteresis in the vortex-wall interaction. As $Re_s \to \infty$ in the Serrin problem (Section 2), we have the asymptotic solution for flow pattern B in Figure 2:

$$\psi = \psi_s x/x_s, \Gamma = 0 \quad \text{for } 0 \le x < x_s$$

and

$$\psi = -Re_s\left\{x_s(1-x)[(2-x_s)x - x_s]/\left(1-x_s^2\right)\right\}^{1/2},$$

$$\Gamma = Re_s \quad \text{for } x_s < x < 1,$$

where

$$\psi_s = Re_s x_s P^{1/2},\ P = (1-x_s)/(1+x_s).$$

As x_s varies from 1 to 0, P changes from 0 to 1 for two-cell flows. For the same range of P, Serrin (1972) proved the existence of one-cell descending flows (flow pattern A in Figure 2). Therefore, there are two solutions—descending

and two-cell—for the same Re_s and P. The reason for this nonuniqueness is similar to that for the free half-line vortex. The flow force J of the annular jet fanning away along the conical surface, $x = x_s$, essentially balances force F_z (see Figure 1, but F_z is directed downward here), i.e. $F_z \approx J$. The physical explanation for the J maximum (near fold C) has already been discussed.

The conical models not only elucidate the mechanism of hysteresis but also reveal another interesting feature concerning the dependence of the Bernoulli head $H(=p + \rho v^2/2)$ and circulation $\Gamma_d(=\nu Re_s)$ on the Stokes stream function Ψ. As $Re_s \to \infty$ for a fixed x_s, the analytic solutions yield the limiting relations,

$$H = p_\infty, \Gamma = 0 \quad \text{for } \Psi < 0 \quad \text{and} \quad H = p_\infty + \frac{1}{2}\rho\Gamma_d^4\,\Psi^{-2},$$

$$\Gamma = Re_s \quad \text{for } \Psi > 0, \tag{4}$$

$$H = p_\infty, \quad \Gamma = 0 \quad \text{for } \Psi > 0 \quad \text{and} \quad H = p_\infty + \frac{1}{2}\rho\Gamma_d^4\Psi^{-2}x_s^2(1+x_s)^{-2},$$

$$\Gamma = Re_s \quad \text{for } \Psi < 0, \tag{5}$$

for the free-space (Equation 4) and vortex-wall (Equation 5) problems. For inviscid steady axisymmetric flows, the governing equation in cylindrical coordinates (r_c, z) is

$$r_c\partial/\partial r_c\left(r_c^{-1}\partial\Psi/\partial r_c\right) + \partial^2\Psi/\partial z^2 = r_c^2 dH/d\Psi - \Gamma d\Gamma/d\Psi, \tag{6}$$

which is often referred to as the Bragg-Hawthorne or Squire-Long equation [although, as Goldshtik & Hussain (1998) pointed out, Meissel (1873) used Equation 6 significantly earlier]. Functions $H(\Psi)$ and $\Gamma(\Psi)$ are defined by inflow boundary conditions outside but are undetermined inside a recirculatory zone.

Some inviscid theories of vortex breakdown involve conjectures that (*a*) $H(\Psi)$ and $\Gamma(\Psi)$ can be analytically continued (Benjamin 1962), or (*b*) flow stagnates in the recirculatory zone (Keller et al 1985). As follows from Equations 4 and 5, $H(\Psi)$ and $\Gamma(\Psi)$ have jumps at $\Psi = 0$, the boundary of recirculatory zone; this contradicts (*a*). Further, the solutions show that swirl is absent, but the meridional motion does occur inside the recirculation zone; this contradicts (*b*). Thus (*a*) and (*b*) both are invalid for the swirling flows treated above.

Now we consider an effect accompanying helical vortex breakdown and occurring in many other flows: loss of axial symmetry.

6. AXISYMMETRY BREAKING

Instability with respect to azimuthal disturbances typically occurs in radially diverging flows and is possibly one of the first documented in the literature.

Thompson (1855) observed the spreading of alcohol (introduced by a capillary tube) from the center of the water surface in a wine glass. He reports "by the motion of the powder, one, two, three, or many radial streams flowing outwards from the middle, and other return streams or eddies flowing backwards to the margin of the patch." Pshenichnikov & Yatsenko (1974) repeated this experiment (unaware of the Thompson observation) and photographed the flow patterns. It is interesting that a motivation for their study was the Bratukhin & Maurin (1967) solution, which describes the axisymmetric Marangoni convection induced by a point source of surfactant. However, the experiment by Pshenichnikov & Yatsenko reveals that the flow is not axisymmetric even for small flow rates. As the flow rate gradually increases, the number of eddies changes from 2 to 10, and then the motion becomes unsteady.

This kind of instability is essentially common to the Marangoni convection and other diverging flows. Its mechanism is inertial: If velocity along a radial line becomes larger than that in the ambient fluid, then pressure decreases along this line (according to the Bernoulli integral for an inviscid fluid). This pressure drop attracts the ambient fluid, whereupon the velocity difference between this and other locations increases. Such a positive feedback triggers the formation of jets and wide inflow regions, while viscous diffusion and dissipation are stabilizing factors.

The manifestation of this mechanism is especially impressive in the Jeffery-Hamel flow. The Jeffery-Hamel solution, modeling the unidirectional diverging flow in a plane diffuser, exists for small, but not large, $Re = Q/\nu$, where Q is the flow rate (Batchelor 1967). This striking fact results from a fold catastrophe (merging and disappearance of two solutions) at $Re = Re_{\rm f}$ (Hooper et al 1982). For $Re < Re_{\rm f}$, this flow becomes unstable with respect to steady (Dennis et al 1997) and oscillating (McAlpine & Drazin 1998) disturbances. New solutions resulting from the instability have both inflow and outflow regions. Symmetry breaking of the Jeffery-Hamel flow is a specific manifestation of the azimuthal instability.

The instability analysis is simplest for the point source (which can be viewed as the limiting case of the Jeffery-Hamel flow, without the walls, when the diffuser angle is increased up to 2π). Goldshtik et al (1991) found that the planar vortex-source is unstable, resulting in bifurcation of the two-dimensional spiral NSE solutions obtained by Oseen (1927). This instability problem (both linear and nonlinear) allows an analytical solution. In particular, the critical values of $Re = r{\rm v}_{\rm r}/\nu$ and $Re_{\rm s} = r{\rm v}_\phi/\nu$ satisfy the relation, $m^2 Re_{\rm s}^2 = (Re+4)^2(2Re + 4 - m^2)$. Shusser & Weihs (1995, 1996) generalized the linear stability study of the vortex-source to three-dimensional disturbances.

Since the bifurcation is subcritical, the Oseen solutions are also unstable. In contrast, bifurcation of nonaxisymmetric solutions appears supercritical

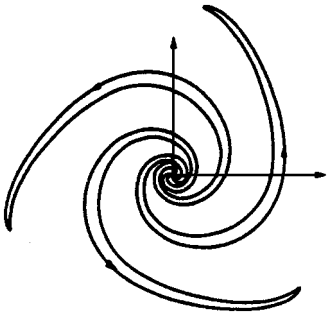

Figure 10 Three-branch vortex, bifurcating from a planar vortex-source.

for the Marangoni convection and for a number of other three-dimensional flows. Moreover, there is a bifurcation cascade corresponding to the subsequent halving of length scales of the disturbance motion (Shtern & Hussain 1994); this cascade is similar to the (inverse) Feigenbaum and the Richardson-Kolmogorov cascades. Thus the nonaxisymmetric Marangoni convection observed by Thompson results from the divergent instability.

Figure 10, resembling spiral galaxies, depicts a three-branch vortex resulting from the divergent instability (Goldshtik et al 1991). One may speculatively view the divergent instability as the simplest mechanism triggering the development of spiral branches of galaxies. The rotating disk of a galaxy acts as a centrifugal pump forcing a fanning, swirling jet of the ambient gas. Such a jet is subject to the divergent instability even adjacent to a no-slip plane.

To demonstrate this feature, we return to the vortex-wall interaction (Figure 1) and consider the instability of this flow with respect to steady helical disturbances. First, we report a new result that the Goldshtik (1960) solution ($F_z = 0$) is unstable with respect to the $m = 1$ mode for $Re_s > Re_{cr} = 5.064$. The neutral disturbance is proportional to $\exp(i\phi - i\alpha_i \ln r)$ with $\alpha_i = 3.047$. Thus, the flow becomes unstable at smaller Re_s than that for the collapse, $Re_{co} = 5.53$.

When the axial force is directed toward the wall and $Re_s \to \infty$, a swirling jet develops fanning along the wall (*inset A* in Figure 2). Such a three-dimensional boundary layer is unstable to helical disturbances. Figure 11 (Shtern & Dallmann 1995) shows the neutral curves for the azimuthal wave number $m = 2, \ldots, 7$. The smallest critical value of $Re_s = Re_{scr} = 63$ corresponds to $m = 3$, while the smallest value of $Re_m = Re_{mcr} = 71$ corresponds to $m = 2$ (note that the $m = 1$ disturbances do not cause the instability here). Fold F and separation S curves seem to merge within the accuracy of the drawing in Figure 11 (note that *curves F* and *0* in Figure 2 merge as $k^{-2} \to 0$). The inset shows separation profiles of swirl γ and radial W' velocities in the limit

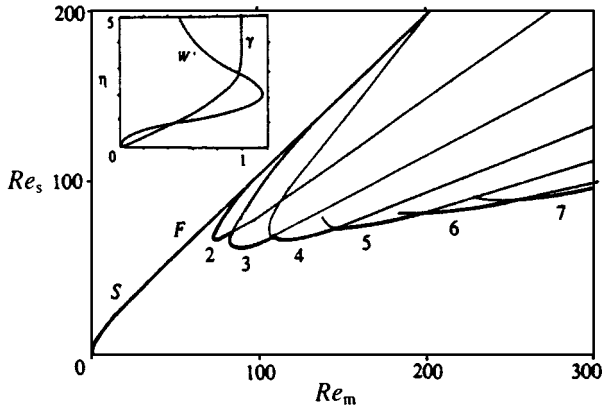

Figure 11 Map of the divergent instability of a wall swirling jet. *Inset* shows profiles of swirl and radial W' velocities. The main plot shows fold F and separation S curves (*coincident*), and neutral curves for azimuthal wave number $m = 2, \ldots, 7$.

$Re_s \to \infty$; γ and W' are normalized with $\gamma(\infty)$, and $\eta = x\,Re_s$ is the distance from the wall. Near the wall, the radial velocity reaches its maximum v_{rm}, and $Re_m = r v_{rm}/\nu$.

The divergent instability seems to explain an experiment by Joukovsky (conducted in 1911, published in 1937, and recently repeated by Vladimirov 1994). A small propeller positioned on the axis between two parallel, fixed disks with a small central orifice generates a fanning, swirling flow. Although the geometry and forcing are nearly axisymmetric, the flow has a few spiral branches depending on parameter values. Note that the divergent instability of the conical wall jet is similar to that observed for flow over a rotating disk, where the steady secondary state develops having m spiral branches (Gregory et al 1955). Also, there is a limited analogy between the divergent and the cross-flow instabilities over a swept wing (Malik & Chang 1994): Both cause the development of steady streamwise vortices.

At first sight, the secondary solutions, resulting from the divergent instability, seem to contradict dimensional analysis. Consider the planar vortex-source, where the given quantities—flow rate, circulation, and viscosity—have the same dimension and thus cannot provide any lengthscale. However, the secondary flow depends on $\chi = m\phi + \alpha \ln(r/r_0)$, where r_0 serves to make the argument of logarithm dimensionless. A change in r_0 merely causes the secondary flow to turn around the origin. Since there is no preferred azimuthal angle ϕ in the problem formulation, any shift in ϕ is admissible, and thus any value of r_0 can be chosen.

The role of r_0 is more significant in axisymmetric three-dimensional flows, which bifurcate from the solution described by Equation 2 and are periodic with respect to $\ln(r/r_0)$ (Shtern & Hussain 1998): A change in r_0 causes a shift of the oscillating solution in the radial direction. In both cases, r_0 is a hidden parameter that governs a phase shift. [A recent theory of cosymmetry (Yudovich & Kurakin 1997) provides the mathematical background for bifurcation of a solution family depending on a hidden parameter.] The phase in practical flows is specified by conditions outside the similarity region. While passing through its similarity region, the flow "remembers" the phase as well as conserved quantities, such as flow rate and momentum. It is typical that the phase is a free parameter of periodic solutions (e.g. for Taylor vortices and thermal-convection rolls) but is specified near endwalls in confined flows. The role of r_0 becomes important indeed for transient solutions switching between primary and secondary steady states.

7. SWITCHING BETWEEN FLOW STATES

Now we consider transitions between steady flow states induced by swirl bifurcation (Section 3), fold catastrophes (Section 5), and azimuthal instability (Section 6). Amplitude equations of Ginzburg-Landau type govern spatiotemporal evolution of instability modes in the vicinity of $Re_{\rm cr}$. To deduce these equations, it is helpful first to transform NSE by introducing the following dependent and independent variables:

$$u(x,\phi,\xi,\tau) = \mathrm{v_r}\, r/\nu, \quad y(x,\phi,\xi,\tau) = \mathrm{v}_\theta r \sin\theta/\nu,$$
$$\Gamma(x,\phi,\xi,\tau) = \mathrm{v}_\phi\, r \sin\theta/\nu, \quad q(x,\phi,\xi,\tau) = (p-p_\infty)r^2/(\rho\nu^2),$$
$$\xi = \ln(r/r_0), \quad x = \cos\theta, \quad \tau = \nu t/r_0^2. \tag{7}$$

Our idea behind this transformation is to exploit the conical similarity of the basic flow in order to simplify the stability analysis. In particular, despite the strong nonparallelism of conical flows, the transformation described by Equation 7 allows the exact reduction of the linear stability problem to ODE, thus extending the advantages of the similarity approach to nonsimilar disturbances.

Govindarajan & Narasimha (1995) have developed an analogous technique using similarity variables for the stability study of Falkner-Skan flows, enabling them to more precisely take into account nonparallel effects. Since the Falkner-Skan similarity is a feature of the boundary layer equations but not of NSE, this approach is approximate—in contrast to the present approach, where the reduction, suitable for any conical flow, is exact—an important difference, which nevertheless disappears for unsteady disturbances.

Terms such as $\exp(2\xi)\partial u/\partial\tau$ are present in the transformed NSE, and therefore the normal modes $\sim \exp(\alpha\xi)$ cannot be applied for infinitesimal disturbances. This makes the temporal stability analysis significantly more difficult than that for steady disturbances. This is overcome here with the help of a small-parameter expansion in the vicinity of $Re = Re_{\rm cr}$ for the instabilities discussed. Since neutral disturbances are steady, the temporal evolution is slow for $Re = Re_{\rm cr} + \varepsilon$ ($|\varepsilon| \ll 1$); this allows the use of a weakly unsteady approach, including weakly nonlinear effects. Shtern & Hussain (1998) developed one such small-parameter technique and derived the amplitude equations for the swirl bifurcation in the form

$$A_{\rm T} = \exp(-2\xi)[\gamma A - \delta|A|^2 A + \varepsilon^{-1}(A_{\xi\xi} - \beta A_\xi)],$$

and for the fold catastrophe in the form

$$A_{\rm T} = \exp(-2\xi)[\gamma A - \delta A^2 + \varepsilon^{-1}(A_{\xi\xi} - \beta A_\xi)],$$

which differ only by the nonlinear terms. Here A is the disturbance amplitude, $T = \varepsilon\tau$ is the "slow" time, and the subscripts indicate differentiation; constants β, γ, and δ follow from the expansion.

The amplitude equations, involving the second derivative with respect to ξ, require two boundary conditions, e.g. at $r = r_{\rm i}$ and $r = r_{\rm o}$. These conditions provide a lengthscale, which is absent in similarity solutions. Thus the approach resolves the lengthscale paradox (see Section 6) and also describes the complete transition between steady flow states.

Detailed stability studies of the swirl and fold bifurcations reveal that the switching disturbances grow monotonically with time during transition from the primary to the secondary steady flow for $Re > Re_{\rm cr}$. These disturbances do not reveal a wavelike character but grow with time at any fixed observation point of the similarity region, i.e. the instability is absolute (Huerre & Monkewitz 1990).

8. SUMMARY AND FUTURE WORK

We have highlighted some intriguing features of swirling flows—collapse, swirl generation, vortex breakdown, hysteresis, and axisymmetry breaking—of both fundamental and practical interest. Further, we have shown how simple models provided by conical similarity solutions help us to understand the mechanisms of these effects.

The singularity development in NSE solutions (collapse) corresponds to the strong accumulation of axial and angular momenta observed in tornadoes and flows over delta wings. Swirl bifurcation in similarity models explains the

threshold character of swirl development in capillary and electro-vortex flows. Analytical solutions for fold catastrophes reveal why there are so few stable states and why the jump transitions between the states occur—features typical of tornadoes and of flows over delta wings and in vortex devices. Finally, the divergent instability explains such effects as the splitting of a tornado and the development of spiral branches in free and near-wall swirling flows. Many important questions still remain unanswered, and certain results need to be extended and improved. Here we list some topics for further exploration.

1. An explanation of collapse in open conical flows, e.g. modeling cosmic jets, Marangoni convection, and electro-vortex flows. To achieve this, it is necessary to study asymptotic features of the corresponding confined flows as the flow region expands to infinity.

2. An explanation of the difference between the $v \sim 1/r$ viscous jets and the *r*-independent inviscid jets.

3. Bifurcation character (sub- or supercritical) of the divergent instability. Of particular interest would be whether a branching helical vortex exists for $Re_s > Re_{co}$ in the vortex-wall problem.

4. Whether chaotic motion develops near intersection points of the neutral curves (e.g. in Figure 11).

5. Scaling features of turbulence in the far field of self-preserving jets.

6. Effects of swirl in compressible flows with applications to flame stabilization in scram jets and vortex combustion chambers.

7. Explanation and modeling of the Ranque effect by similarity solutions.

8. An explanation of the antidiffusion phenomenon (Husain et al 1995).

9. The development of a matching technique for conical and outer solutions, in order to model complex swirling flows with a number of recirculatory zones (as in Figure 7).

ACKNOWLEDGMENTS

The authors dedicate this paper to the memory of Mikhail Goldshtik. Preparation of this manuscript was partially supported by NSF Grant CTS-9622302.

Literature Cited

Althaus W, Brücker C, Weimer M. 1995. Breakdown of slender vortices. In *Fluid Vortices*, ed. SI Green, pp. 373–426. Dordrecht: Kluver Academic

Arnol'd VI. 1984. *Catastrophe Theory*. Berlin: Springer-Verlag

Bailey AG. 1988. *Electrostatic Spraying in Liquids*. New York: Wiley & Sons

Batchelor GK. 1967. *An Introduction to Fluid Dynamics*. Cambridge, UK: Cambridge Univ. Press

Batchelor GK, Gill AE. 1962. Analysis of stability of axisymmetric jets. *J. Fluid Mech.* 14:529–51

Benjamin TB. 1962. Theory of vortex breakdown phenomena. *J. Fluid Mech.* 14:593–629

Beran PS, Culick FEC. 1992. The role of nonuniqueness in the development of vortex breakdown in tubes. *J. Fluid Mech.* 242:491–527

Bojarevics V, Freibergs JA, Shilova EI, Shcherbinin EV. 1989. *Electrically Induced Vortical Flows*, pp. 136–38. Dordrecht: Kluver Academic

Braginsky SI. 1964. Self-excitation of magnetic field during the motion of highly conducting fluid. *Sov. Phys. JETP* 48:1084–98

Bratukhin YK, Maurin LM. 1967. Thermocapillary convection in a fluid filling a half-space. *J. Appl. Math. Mech.* 31:605–8

Buntine JD, Saffman PG. 1995. Inviscid swirling flows and vortex breakdown. *Proc. R. Soc. London Ser. A* 448:1–15

Burggraf OR, Foster MR. 1977. Continuation or breakdown in tornado-like vortices. *J. Fluid Mech.* 80:685–704

Cooke JC. 1952. On Pohlgausen's method with application to a swirl problem of Taylor. *J. Aerosp. Sci.* 19:486–90

Cowling TG. 1934. The magnetic field of sunspots. *Monthly Notes, R. Astron. Soc.* 94:39–48

Davies-Jones RP. 1983. Tornado dynamics. In *Thunderstorms: A Social, Scientific and Technological Documentary*, ed. K Kessler, 2:297–361. Norman: Univ. Oklahoma Press

Delbende T, Chomas JM, Huerre P. 1998. Absolute/convective instabilities in the Batchelor vortex: a numerical study of the linear response. *J. Fluid Mech.* 355:229–54

Dennis SCR, Banks WHH, Drazin PG, Zaturska MB. 1997. Flow along a divergent channel. *J. Fluid Mech.* 336:183–202

Earnshow PB. 1961. An experimental investigation: the structure of a leading-edge vortex. *Aeronaut. Res. Counc.*, Rep. 22

Escudier M. 1984. Observations of the flow produced in a cylindrical container by a rotating endwall. *Exp. Fluids* 2:189–96

Escudier M. 1987. Confined vortices in flow machinery. *Annu. Rev. Fluid Mech.* 19:27–52

Fenn JB, Mann M, Meng CK, Wong CF, Whitehouse C. 1989. Electrospray ionization for mass spectrometry of large biomolecules. *Science* 246:64–71

Fernández de la Mora J. 1992. The effect of charge emission from electrified liquid cones. *J. Fluid Mech.* 243:561–74

Fernández de la Mora J, Fernández-Feria R, Barrero A. 1991. Theory of incompressible conical vortices at high Reynolds numbers. *Bull. Am. Phys. Soc.* 36:2619

Fernández-Feria R, Fernández de la Mora J, Barrero A. 1995. Solution breakdown in a family of self-similar nearly inviscid axisymmetric vortices. *J. Fluid Mech.* 305:77–91

Fulton CD. 1950. Ranque's tube. *Refr. Eng.* 58:473–79

Funakoshi M, Inoue S. 1988. Surface waves due to resonant horizontal oscillation. *J. Fluid Mech.* 192:219–47.

Gelfgat AY, Bar-Yoseph PZ, Solan A. 1996. Stability of confined swirling flow with and without vortex breakdown. *J. Fluid Mech.* 311:1–36

Goldshtik MA. 1960. A paradoxical solution of the Navier-Stokes equations. *J. Appl. Math. Mech.* 24:610–21

Goldshtik MA. 1979. On swirling jets. *Fluid Dyn.* 14:19–26

Goldshtik MA. 1990. Viscous-flow paradoxes. *Annu. Rev. Fluid Mech.* 22:441–72

Goldshtik M, Hussain F. 1997. The nature of inviscid vortex breakdown. *Phys. Fluids* 9:263–65.

Goldshtik M, Hussain F. 1998. Analysis of inviscid vortex breakdown in a semi-infinite pipe. *Fluid Dyn. Res.* 23:189–234

Goldshtik M, Hussain F, Shtern V. 1991. Symmetry breaking in vortex source and Jeffery-Hamel flows. *J. Fluid Mech.* 232:521–66

Goldshtik MA, Shtern VN. 1990. Collapse in conical viscous flows. *J. Fluid Mech.* 218:483–508

Goldshtik MA, Shtern VN. 1993. Axisymmetric hydromagnetic dynamo. In *Advances in Turbulent Studies*, ed. H Branover, Y Unger. *Progr. Astronaut. Aeronaut.* 149:87-102. Washington: AIAA Inc

Goldshtik MA, Shtern VN, Zhdanova EM. 1984. Onset of self-rotation in a submerged jet. *Sov. Phys. Dokl.* 277:815–18

Goldshtik MA, Yavorsky NI. 1989. On the flow between a porous rotating disk and plane. *J. Fluid Mech.* 207:1–42

Govindarajan R, Narasimha R. 1995. Stability of spatially developing boundary layers in pressure gradients. *J. Fluid Mech.* 300:117–47

Gregory N, Stuart JT, Walker WC. 1955. On the stability of three dimensional boundary layer with application to the flow due to a rotating disk. *Philos. Trans. R. Soc. London Ser. A* 248:155–99

Guilloud JC, Arnault J, Discrescendo C. 1973. Étude d'une nouvelle famille des solutions de Navier-Stokes. *J. Mech.* 12:47–74

Hall MG. 1972. Vortex breakdown. *Annu. Rev. Fluid Mech.* 4:125–218

Hayati I, Bailey A, Tadros TF. 1986. Mechanism of stable jet formation in electrohydrodynamic atomization. *Nature* 319:41–43

Hooper AP, Duffy BR, Moffat HK. 1982. Flow of fluid of nonuniform viscosity in converging and diverging channels. *J. Fluid Mech.* 117:283–304

Huerre P, Monkewitz PA. 1990. Local and global instabilities in spatially developed flows. *Annu. Rev. Fluid Mech.* 22:473–537

Husain HS, Hussain F, Goldshtik M. 1995. Anomalous separation of homogeneous particle-fluid mixtures: further observations. *Phys. Rev. E* 52:4909–23

Joukovsky NE. 1937. *Collected papers*, Vol. 6. Moscow: ONTI (In Russian)

Kawakubo M, Tsuchia Y, Sugaya M, Matsumura K. 1978. Formation of a vortex around a sink: a kind of phase transition in a nonequilibrium open system. *Phys. Lett. A* 68:65–66

Keller JJ, Egli W, Exley W. 1985. Force- and loss-free transitions between flow states. *Z. Angew. Math. Phys.* 36:854–89

Lada CJ. 1985. Cold outflows, energetic winds, and enigmatic jets around young stellar objects. *Annu. Rev. Astron. Astrophys.* 23:267–317

Landau LD. 1944. On exact solution of the Navier-Stokes equations. *Dokl. Akad. Nauk SSSR* 43:299–301

Leibovich S. 1978. The structure of vortex breakdown. *Annu. Rev. Fluid Mech.* 10:221–46

Leibovich S. 1984. Vortex stability and breakdown: survey and extension. *AIAA J.* 22: 1192–206

Long RR. 1961. A vortex in an infinite viscous fluid. *J. Fluid Mech.* 11:611–23

Lopez JM. 1994. On the bifurcation structure of axisymmetric vortex breakdown in a constricted pipe. *Phys. Fluids* 6:3683–93

Lopez JM. 1998. Characteristics of endwall and sidewall boundary layers in a rotating cylinder with a differentially rotating endwall. *J. Fluid Mech.* 359:49–79

Lowson MV. 1964. Some experiments with vortex breakdown. *J. R. Aeronaut. Soc.* 68: 343

Malik M, Chang CL. 1994. Crossflow disturbances in three-dimensional boundary layers: nonlinear development, wave interaction, and secondary instability. *J. Fluid Mech.* 268:1–36

McAlpine A, Drazin PG. 1998. On the spatiotemporal development of small perturbations of Jeffery-Hamel flows. *Fluid Dyn. Res.* 22: 123–38

Meissel E. 1873. Über den Ausfluss der Wasser aus Gefässen in zwei besonderen Fällen nach Eintritt des Beharrungszustandes. *Arch. Math. Phys.* 55

Menke M, Gursul I. 1997. Unsteady nature of leading edge vortices. *Phys. Fluids* 9:2960–66

Muylaert IM. 1980. Effect of compressibility on vortex bursting on slender delta wings. *VKI Proj. Rep. 1980-21*

Ogawa A. 1992. *Vortex Flows*, pp. 297–361. Boca Raton: CRC Press

Olendraru C, Sellier A, Rossi M, Huerre P. 1996. Absolute/convective instability of the Batchelor vortex. *C. R. Acad. Sci. Paris* IIb:153–59

Oseen CW. 1927. Exacte Lösingen der hydrodynamischen Differential-gleichungen. *Arkiv fur Matematik, Astr. Fysik* I (14):1–14; II (22):1-9

Paull R, Pillow AF. 1985. Conically similar viscous flows. Part 3. Characterization of axial causes of swirling flows and one-parameter flow generated by a uniform half-line source of kinematic swirl angular momentum. *J. Fluid Mech.* 155:359–80

Peckham DH, Atkinson SA. 1957. Preliminary results of low speed wind tunnel tests on a Gothic wing of aspect ratio 1.0. *Aeronaut. Res. Counc. Tech. Rep.* CP-508, TN No. Aero. 2504

Pshenichnikov AF, Yatsenko SS. 1974. Convective diffusion from localized source of surfactant. In *Hydrodynamics* V (scientific papers of Perm Univ.), pp. 175–81 (In Russian)

Rusak Z, Wang S, Whiting CH. 1998. The evolution of a perturbed vortex in a pipe to axisymmetric vortex breakdown. *J. Fluid Mech.* 366:211–37

Saffman PG. 1992. *Vortex Dynamics*. Cambridge, UK: Cambridge Univ. Press

Sagalakov AM, Yudintsev AY. 1992. Self-oscillations of MHD flows in an annulus pipe in the presence of the axial magnetic field. *Magnetohydrodynamics* 28:7–12

Sarpkaya T. 1971. Vortex breakdown in swirling conical flows. *AIAA J.* 9:1792–99

Sarpkaya T. 1995. Turbulent vortex breakdown. *Phys. Fluids* 7:2301–3

Schlichting H. 1933. Laminaire Strahlausbreitung. *Z. Angew. Math. Mech.* 13:260–3

Schneider W, Zauner R, Bohm H. 1987. The recirculatory flow induced by a laminar axisymmetric jet issuing from a wall. *Trans. ASME I J. Fluid Eng.* 109:237–41

Serrin J. 1972. The swirling vortex. *Philos. Trans. R. Soc. London Ser. A* 271:325–60

Shtern V, Barrero A. 1995. Bifurcation of swirl in liquid cones. *J. Fluid Mech.* 300:169–205

Shtern V, Borissov A, Hussain F. 1997. Vortex sink with axial flow: solution and applications. *Phys. Fluids* 9:2941–59

Shtern V, Dallmann U. 1995. Asymptotic stability of turbulent swirling jets fanning out along a plane. In *Asymptotic methods for Turbulent Shear Flows at High Reynolds Numbers*, ed. K Gersten, pp. 267-80. Dordrecht: Kluver Academic

Shtern V, Hussain F. 1994. Bifurcation cascade in a diverging flow. In *Nonlinear Stability of Nonparallel Flows*, ed. SP Lin, WRC Philips, DT Valentine, pp. 449-58. Berlin: Springer-Verlag

Shtern V, Hussain F. 1996. Hysteresis in swirling jets. *J. Fluid Mech.* 309:1–44

Shtern V, Hussain F. 1998. Instabilities of conical flows causing steady bifurcations. *J. Fluid Mech.* 366:33–85

Shusser M, Weihs D. 1995. Stability analysis of source and sink flows. *Phys. Fluids* 7:2345–54

Shusser M, Weihs D. 1996. Stability of source-vortex and doublet flows. *Phys. Fluids* 8: 3197–99

Sozou C. 1971. On fluid motion induced by an electric current source. *J. Fluid Mech.* 46:25–32

Sozou C, Wilkinson LC, Shtern VN. 1994. On conical swirling flows in an infinite fluid. *J. Fluid Mech.* 276:261–71.

Squire HB. 1952. Some viscous fluid flow problems. 1. Jet emerging from a hole in a plane wall. *Philos. Mag.* 43:942–45

Squire HB. 1956. Rotating fluids. In *Surveys in Mechanics*, ed. GK Batchelor, RM Davies, pp. 139-61. Cambridge, UK: Cambridge Univ. Press

Taylor GI. 1950. The boundary layer in the converging nozzle of a swirl atomizer. *Q. J. Mech. Appl. Math.* 3:129–39

Taylor GI. 1964. Disintegration of water drops in an electric field. *Proc. R. Soc. London Ser. A* 280:383–97

Thompson J. 1855. On certain curious motions observable at the surfaces of wine and other alcoholic liquors. *Philos. Mag. Ser.* 4, 10: 330–33

Torrance KE. 1979. Natural convection in the thermally stratified enclosures with localized heating from below. *J. Fluid Mech.* 95:477–95

Trigub VN. 1985. The problem of breakdown of a vortex line. *J. Appl. Math. Mech.* 49:166–71

Vladimirov VA. 1994. Strong asymmetry in swirling flows. In *Proc. 1st Int. Conf. Flow Interaction*, ed. NWM Ko, HE Fiedler, BHK Lee, pp. 366-69. Hong Kong: Hong Kong Univ. Press

Wang CV. 1991. Exact solutions of the steady-state Navier-Stokes equations. *Annu. Rev. Fluid Mech.* 23:159–77

Wang S, Rusak Z. 1997. The dynamics of a swirling flow in a pipe and transition to axisymmetric vortex breakdown. *J. Fluid Mech.* 340:177–223

Werle H. 1963. *La Hoille Blanche* 28:330 (photo reproduced from RL Panton, *Incompressible Flow*, p. 569. New York: Wiley & Sons, 1996)

Wygnanski I, Fiedler H. 1969. Some measurements in the self-preserving jet. *J. Fluid Mech.* 38:577–612

Yatseev VN. 1950. On a class of exact solutions of the viscous fluid motion equations. *Sov. Phys., J. Exp. Theor. Phys.* 20:1031–34

Yih CH, Wu F, Garg AK, Leibovich S. 1982. Conical vortices: a class of exact solutions of the Navier-Stokes equations. *Phys. Fluids* 25:2147–57

Yudovich VI, Kurakin LG. 1997. Bifurcation of the branching of a circle in *n*-parametric family of dynamic systems with cosymmetry. *Chaos* 7:376–86

Zanderbergen PJ, Dijkstra D. 1987. Von Kármán swirling flows. *Annu. Rev. Fluid Mech.* 19:465–91

Zeleny J. 1917. Instability of electrified liquid surface. *Phys. Rev.* 10:1–6

Annual Review of Fluid Mechanics
Volume 31, 1999

CONTENTS